Remaining Useful Life Estimation for LFP Cells in Second-Life Applications

Iván Sanz-Gorrachategui, Pablo Pastor-Flores, Milutin Pajovic, *Member, IEEE*, Ye Wang, Philip V. Orlik, *Senior Member, IEEE*, Carlos Bernal-Ruiz, *Member, IEEE*, Antonio Bono-Nuez, and Jesús Sergio Artal-Sevil

***Abstract*— The increasing deployment of battery storage applications in both grid storage and electric vehicle fields is generating a vast used battery market. These batteries are typically recycled but could be reused in second-life applications. One of the challenges is to obtain an accurate remaining useful life (RUL) estimation algorithm, which determines whether a battery is suitable for reuse and estimates the number of second-life cycles the battery will last. In this article, the RUL estimation problem is considered. We propose several health indicators (HIs), some of which have not been explored before, along with simple yet effective estimation and classification algorithms. These algorithms include classification techniques such as regularized logistic regression (RLR), and regression techniques such as multivariable linear regression (MLR) and multilayer perceptron (MLP). As a more advanced solution, a multiple expert system combining said techniques is proposed. The performance of the algorithms and features is evaluated on a recent lithium iron phosphate (LFP) data set from Toyota Research Institute. We obtain satisfactory results in the estimation of RUL cycles with errors down to 49 root mean square error (RMSE) cycles for cells that live up to 1200 cycles, and 0.24% mean relative error (MRE) for the prediction of the evolution of capacity.**

***Index Terms*— Capacity prediction, lithium iron phosphate (LFP), lithium-ion batteries, remaining useful life (RUL), second-life battery applications.**

I. Introduction

ENERGY storage systems (ESSs) based on lithium-ion cell technologies are becoming the standard for many different storage applications due to the high energy density, high efficiency, and declining manufacturing costs [1], [2]. In addition, they also provide longer service lives than other traditional alternatives, such as lead–acid chemistries, and are less contaminant than nickel-related chemistries such as NiCd [3], [4]. Lithium-ion technologies, such as lithium iron phosphate (LFP), lithium nickel manganese cobalt oxide (NMC), lithium titanate oxide (LTO), or lithium nickel cobalt aluminum oxide (NCA), are some of the most popular lithium-based variants and are the main options used in electric vehicle (EV) applications [5]–[8]. The increasing number of these ESSs due to the expansion of EV is beginning to generate an enormous second-hand battery market, and reusing these batteries is a promising application [9].

Second life of lithium-ion batteries has been studied from an economical, technical, and environmental approach [10]. A common conclusion is that a suitable second-life application for these batteries is low-demanding applications in terms of power requirements and depth of discharge (DoD), such as energy storage in on-grid systems [10]–[12]. However, some key challenges need to be addressed before this becomes a reality, such as estimating the remaining useful life (RUL) of these used batteries. The aging of lithium-ion batteries has been extensively studied and has proven to be a challenging problem [13]–[18]. RUL estimation studies have traditionally been focused on *in situ* applications i.e., estimating the RUL of batteries that are already embedded in an application and monitored, where the main goal is to predict the failure threshold [19]–[24]. In the problem of RUL estimation for second-life applications, knowledge of the past use of the battery is usually required [25].

Regarding the techniques used for the RUL estimation problem, there are two traditional approaches to the problem: model-based analysis and data-driven analysis. While model-based analysis is suitable for battery behavioral models, cell aging is a much more complex process, with many more agents involved. Thus, a data-driven approach is suitable for this task. However, until very recently, publicly available data sets were small [19], [26]. The data set introduced in [27] was published recently (March '19) by researchers of the Toyota Research Institute (TRI) and the Massachusetts Institute of Technology (MIT), and is the largest currently available. This data set contains information on 124 cells, which are cycled until their end of life (EoL), as defined as their capacity falling below 80% of their initial capacity. This provides more than

Manuscript received July 23, 2020; revised December 22, 2020; accepted January 10, 2021. Date of publication February 1, 2021; date of current version February 19, 2021. This work was supported in part by the Fulbright Commission, in part by Regional Strategy for Research and Innovation for Smart Specialization (RIS3) Aragon Government, and in part by the EU Project Sistemas de Almacenamiento Híbridos e Inteligentes (SAHI) under Grant LMP16_18. The Associate Editor coordinating the review process for this article was Dr. Octavian Adrian Postolache. *(Corresponding author: Ye Wang.)*

Iván Sanz-Gorrachategui was with the Mitsubishi Electric Research Laboratories (MERL), Cambridge, MA 02139 USA. He is now with the Electrical and Communication Engineering Department, University of Zaragoza, 50018 Zaragoza, Spain (e-mail: isgorra@unizar.es).

Pablo Pastor-Flores, Carlos Bernal-Ruiz, Antonio Bono-Nuez, and Jesús Sergio Artal-Sevil are with the Electrical and Communication Engineering Department, University of Zaragoza, 50018 Zaragoza, Spain (e-mail: pablop@unizar.es; cbernal@unizar.es; antoniob@unizar.es; jsartal@unizar.es).

Milutin Pajovic was with the Mitsubishi Electric Research Laboratories (MERL), Cambridge, MA 02139 USA. He is now with Analog Devices Inc., Boston, MA 02110 USA (e-mail: micopajovic@gmail.com).

Ye Wang and Philip V. Orlik are with the Mitsubishi Electric Research Laboratories (MERL), Cambridge, MA 02139 USA (e-mail: yewang@merl.com; porlik@merl.com).

Digital Object Identifier 10.1109/TIM.2021.3055791

90 000 full discharge cycles, with several measured features. In the original article, the authors use this data set for RUL prediction purposes, introducing some novel health indicators (HIs). Their focus is the early RUL estimation on a monitored cell before it shows capacity-fade.

This article takes the previous study as a starting point. We use the same data set, but instead, focus on RUL and capacity estimation for second-life applications. We assume that a cell at an unknown moment of its life needs to be evaluated, and through some test cycles, we extract features from processing the measured voltage and charge waveforms. For this purpose, we use some HI that has already been introduced in the literature, together with some less explored indicators. With this set of measurements, we train some simple but effective machine learning algorithms to classify the cells in "long RUL" or "short RUL" classes and predict the exact number of RUL cycles and the future capacity after a set amount of cycles.

This article is organized as follows. In Section II, we discuss different approaches to the RUL estimation problem, and we describe the HI that we use. In Section III, we propose a simple classification algorithm that can cluster short RUL or high RUL batteries with high accuracy. Section IV describes some regression algorithms to estimate the number of remaining cycles of the cells and predict the future capacity in a set amount of cycles. We summarize our conclusions in Section V.

II. Machine Learning Approach

In the literature, the RUL estimation problem has been addressed with different approaches. Data-driven or machine learning approaches are rising in popularity in recent years; however, the lack of convenient and large data sets has hampered progress in this area. The different approaches to address the estimation of RUL of a cell have been traditionally classified into these two categories [19], [28].

1) *Direct Estimation of RUL:* When considering direct estimation, we assume that the capacity is available as a feature for our algorithms. This means that when the cell is not in an online application, we can perform test cycles to obtain the capacity, or when the cell is in an online application that cycles it completely, we can directly measure its capacity without disconnecting it.
2) *Indirect Estimation of RUL:* This type of estimation does not rely on capacity as a feature to determine aging and RUL. It is aimed at industrial applications, where the battery is not cycled completely, and where it is not possible to disconnect cells to measure features.

When studying if a cell is suitable for a second-life application, all the features can be measured through laboratory cycles, thus can be used in a direct estimation algorithm. On the other hand, some features (such as capacity) might not be directly measurable in an industrial application. The focus of this article is the direct estimation of RUL and future capacity, although in Section V we will provide some insight for indirect estimation problems.

We use the data set from [27] since it is the largest publicly available. It contains information from 124 commercial LFP/graphite cells, which were cycled until their EoL. The specific model of the cells is APR18650M1A from A123 Systems, and they have a 1.1 Ah nominal capacity. The cells have variated high-current charge patterns, but they have all been discharged with the same discharge current (4C) along with all their life. During all cycles, the ambient temperature was controlled to be 30 °C. The cell lives range from 170 cycles to 2237 cycles in extreme cases.

In their data collection, waveforms for voltage, temperature, charge, and time were measured for each cycle of each cell. The data set also provides the observed capacity and an estimate of the internal resistance of the cell once for each cycle.

The study in [27] uses this data set and aims to estimate RUL after the 100th cycle of a cell that has been monitored from the beginning of its life, thus using information from its first 100 cycles. In said study, the authors conclude the variance of the difference of the charge (Q) in the discharge waveform between cycles 100 and 10; $\text{var}(\Delta Q_{100-10})$ is a key feature for determining the RUL of the cell.

However, our study is motivated by a different concern, where we have a cell that has been used in a high current, deep cycle application (such as EV), and we would like to determine whether the cell is suitable for another application, by estimating its RUL and its future capacity. Thus, we do not have full information on its past usage, but we can perform some test cycles to the cell to collect data and calculate some useful features. Let us say we perform δ cycles to an already used cell, which is in its ith cycle of life. We can process the feature $\text{var}(\Delta Q_{(i+\delta)-i})$; however, this turns out to be very noisy unless δ is large enough. Making δ bigger helps to solve this issue, but it means wasting life cycles of the cell for testing purposes. For this reason, we consider some other features, presented in Section II-A.

A. Selected Features

Unlike the original study [27], we are going to consider that each cycle in the data set is an example, instead of each cell. This approach is convenient considering our second-life hypothesis: as we do not know what condition a second-hand battery will be in when we receive it, the algorithms need to be trained with cycles of batteries in different moments of their life. Furthermore, this way we increase the data set from 124 cell examples to more than 90 000, which is the total amount of cycles of all the cells. Each example will have its own set of features and will have as output the number of RUL cycles the cell had at that specific cycle. Some of these features, such as the measured capacity and internal resistance, are already provided by the data set for each cycle of each cell. Other features are computed from processing the waveforms of each cycle.

As introduced before, the hypothesis is that we are conducting δ test cycles to an already used cell. This means that for most of the features, we will have available δ measurements, while for some others, we will have available δ–1, as is described below.

1) *Capacity, C [Ah]:* Amount of charge extracted in each full-discharge cycle. Fig. 1(a) shows an example of the evolution of this feature for one of the cells in the data set. Degradation can be seen over the life of the cell, with an accelerated decay near the EoL.

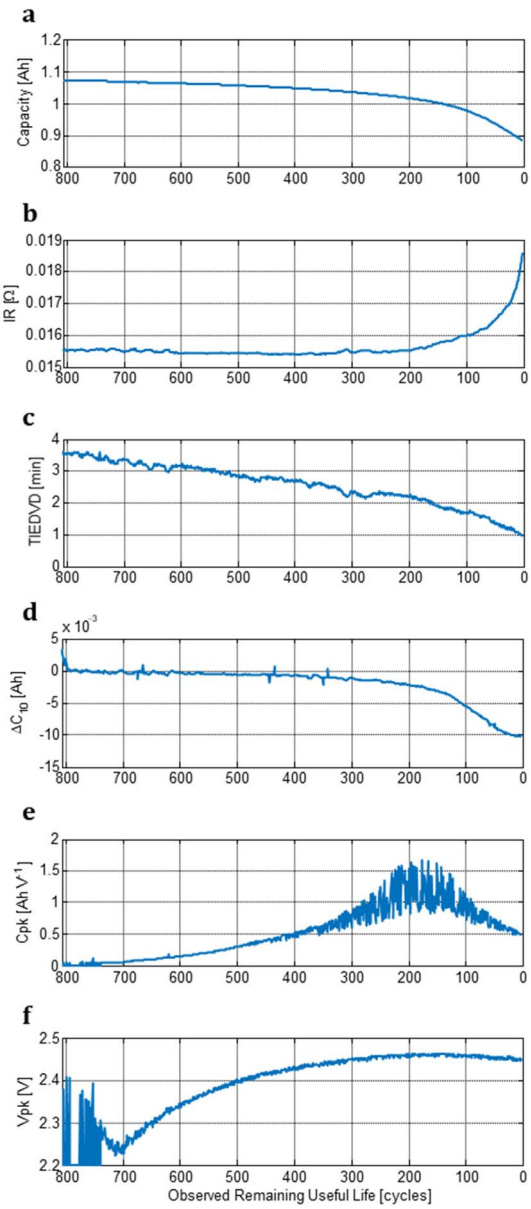

Fig. 1. Feature evolution for one cell versus its life cycles (#100). (a) Capacity evolution. (b) Internal resistance evolution. (c) TIEDVD evolution. (d) ΔC10 Evolution. (e) Capacitance Peak evolution. (f) Voltage at capacitance peak evolution.

2) *Internal Resistance, IR [Ω]:* Internal resistance value. One measurement per cycle is provided in the original data set, obtained by averaging ten current pulses at 80% of State of Charge (SoC). An example of its evolution is shown in Fig. 1(b), where it can be observed how the internal resistance increases abruptly when the cell is near its EoL. Some specific cells with an abnormally high IR value (30% higher than the average) have been taken out as outliers.
3) *Time interval of equal discharging voltage difference (TIEDVD) [min]:* Time lapse between two voltage thresholds ($V_{\max}$, $V_{\min}$) while discharging a constant and known current. Seen in the literature in industrial applications for indirect estimation purposes ([19], [22]) when it is not possible to completely discharge the cell to measure its capacity [e.g., an uninterruptible power supply (UPS)]. This can be used here as another feature obtained from the voltage-time waveforms of each cycle. We have tried different threshold voltages for estimation purposes, and have found that the couple (3.3, 3.15 V) shows good estimation capabilities for this data set. It can be appreciated in Fig. 1(c) how it decreases very linearly with the RUL.
4) *Capacity Fade $\Delta C_\delta[C]$:* Variation in capacity between two cycles separated δ cycles apart. Similarly, as what happened with $\text{var}(\Delta Q_{(i+\delta)-i})$, a greater value for δ improves the prediction capabilities, at expense of aging more the cell for test purposes. We have found that $\delta = 10$ is a good tradeoff in accuracy. Later on, this aspect will be further developed. An example of its evolution is shown in Fig. 1(d). As happens with Capacity and Internal Resistance, in the last hundreds of cycles, its behavior changes drastically.

Besides these features, which have been used previously in the literature, we introduce two new HIs we found for this data set which provide useful information.

1) *Capacitance Peak, Cpk [AhV^{-1}]:* As the cell ages, a small disturbance appears in the low-voltage part of the discharge waveform. It grows until a certain moment in its life and then becomes smoother when the cell is near its EoL. This generates a peak in the cell equivalent capacitance [27], [29]–[32], as seen in Fig. 2. This capacitance peak can be used as another feature. Fig. 1(e) shows how this peak evolves along with cell life, increasing in the first hundreds of cycles, and then decreasing in the last 150 cycles approximately. However, there are some issues with this feature: When the peak is near its maximum, it is a very noisy feature. On the other hand, when the peak is near its minimum (the first 80 cycles of life), the peak cannot be detected correctly.
2) *Voltage at Capacitance Peak, Vpk [V]:* We also use the voltage at which the capacitance peak is observed, as an additional feature, as it varies with cell life. The evolution of this feature is shown in Fig. 1(f). Similar to the case of the Capacitance Peak, it can be seen how in the first 80 cycles of life it cannot be captured correctly.

Similar capacitance peaks obtained with lower discharge currents have been studied before for LFP batteries, and have been used as HIs [27], [32]. However, these approaches aimed to determine degradation mechanisms, and have not been extensively applied to high current waveforms.

Given these processed features, our algorithm aims to estimate.

1) *Remaining Useful Life (RUL) [cycles]:* Number of remaining cycles from the current cycle until EoL. Cells with more than 1300 RUL cycles or with less than 300 RUL cycles have been taken out as outliers since the vast majority of the data set seems to range between 500 and 1200 life cycles. We end up using 113 cells, which add up to more than 80 000 test cycles in the selected data set.

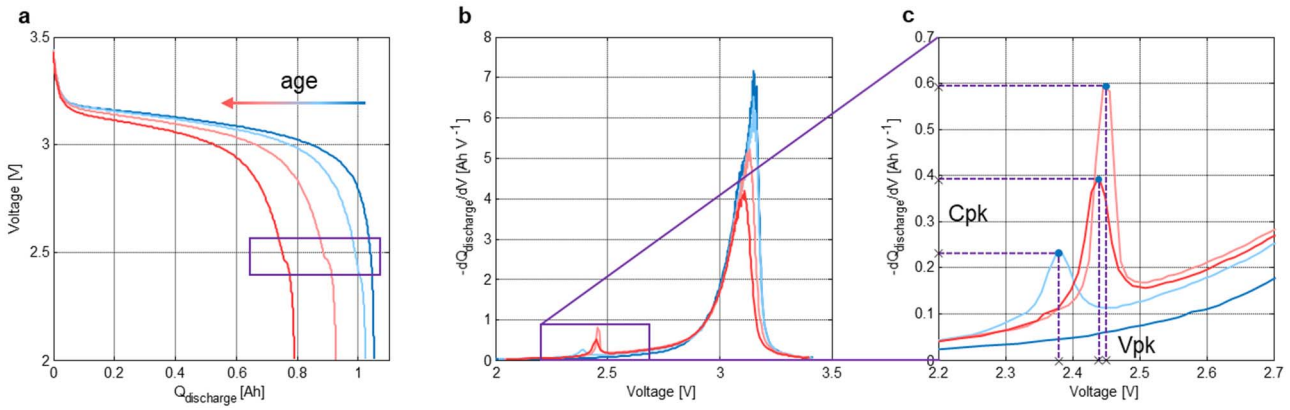

Fig. 2. Capacitance peak advent. (a) Voltage versus charge curve and its variation as the cell ages. (b) Charge derivative to voltage (capacitance), and its variation as the cell ages. (c) Zoomed-in view of the lower voltage part, where the secondary capacitance peak appears.

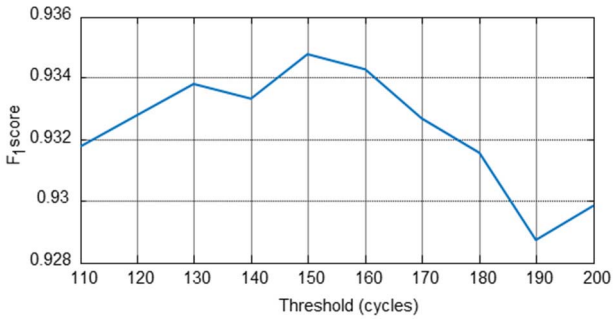

Fig. 3. F_1 score for classification of cells into "short RUL" and "long RUL," with different threshold values.

III. RUL Classification

As discussed in Section II, there is a clear trend in some specific features when the cells are close to their EoL. The features Capacity, Internal Resistance, and Capacity Fade change drastically when the cell is in its last 100 to 200 cycles. In this interval, the "aging knee" of the Capacity curve takes place [10], and according to [33], batteries below this life horizon should not be considered for a second-life application. This change of behavior also suggests the possibility of training an algorithm to determine whether a cell is in this EoL region.

Thus, we have defined the classes "Short RUL cell" and "Long RUL cell" to classify those cells below or above this threshold (in remaining cycles). To establish the best threshold between the classes, an initial classification algorithm (logistic regression) has been tested. We have obtained the F1 score for different threshold values with this algorithm, and the best value has been established in 150 RUL cycles (Fig. 3).

A. Classification Algorithm

The algorithm that has been proposed for the classification task is regularized logistic regression (RLR). The model that this algorithm tries to fit is given by the expression in the following equation:

$$\hat{y}(\boldsymbol{x}, \boldsymbol{w}) = \frac{1}{1 + e^{-\boldsymbol{w}^T \boldsymbol{x}}} \tag{1}$$

where the predicted output $\hat{y}$ is the probability for the cell to belong to "Short RUL cell" and "Long RUL cell" classes, respectively, $\boldsymbol{x}$ is an n-dimensional feature array, and $\boldsymbol{w}$ is an n-dimensional weight array. The output class is obtained by thresholding $\hat{y}$ with 0.5, with 0 meaning "short RUL" and 1 meaning "long RUL."

The algorithm fits $\boldsymbol{w}$ by minimizing the cost function J in the following equation:

$$J(\boldsymbol{w}) = \frac{1}{m} \sum_{i=1}^{m} (E(\boldsymbol{x}_i, \boldsymbol{w}, y_i)) + \lambda \sum_{j=1}^{n} \boldsymbol{w}_j^2. \tag{2}$$

In this equation, the first term represents the traditional cost function for conventional logistic regression, and the second term represents the Ridge regularization function that makes the algorithm less prone to overfitting. The parameter λ weights the regularization term and is set in the training. The parameter m represents the number of examples in the training data set and the error function $E(\boldsymbol{x}_i, \boldsymbol{w}, y_i)$ represents the traditional cost function used for conventional logistic regression, given by the following equation:

$$E(\boldsymbol{x}_i, \boldsymbol{w}, y_i) = -y_i \log(\hat{y}(\boldsymbol{x}_i, \boldsymbol{w})) - (1 - y_i) \log(1 - \hat{y}(\boldsymbol{x}_i, \boldsymbol{w})). \tag{3}$$

B. Determining the Optimal Number of Test Cycles δ

The number of test cycles δ has been introduced before as a means of obtaining more measurements for the features of the cell under test. Specifically, a larger δ allows us to gather more information about the RUL of the cell according to (4). A specific number of cycles δ gives us δ measurements for each feature except ΔC, and $\delta - 1$ measurements for ΔC

$$n_{\text{measurements}} = 6\delta - 1. \tag{4}$$

This comes at expense of reducing the RUL for test purposes. Thus, there is a tradeoff between δ and the success rate achieved. To determine the best δ, logistic regression has been used as the initial algorithm for the classification task, due to its simplicity. We have tested different sets of variables, including and excluding some of them and applying certain

TABLE I
FEATURES USED IN THE ALGORITHMS

Feature	Samples used as inputs	Nº of samples
C	C_δ	1
ΔC	$[\Delta C_2, \ldots \Delta C_\delta]$	δ-1
Vpk, Cpk	$[Vpk_1/\log_{10}(Cpk_1), \ldots Vpk_\delta/\log_{10}(Cpk_\delta)]$	δ
IR	$[IR_1, \ldots IR_\delta]$	δ
TIEDVD	$[TIEDVD_1, \ldots TIEDVD_\delta]$	δ

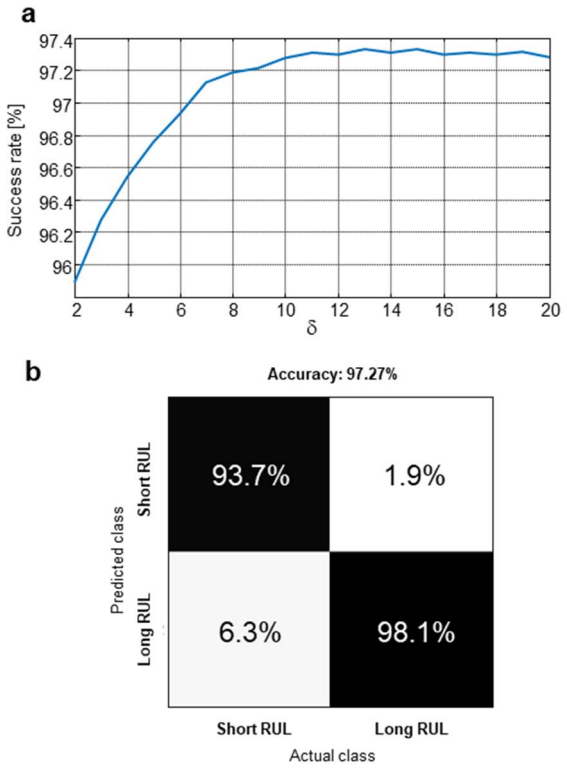

Fig. 4. Results for the RLR algorithm. (a) Success rate for each δ value. (b) Confusion matrix for the case of $\delta = 10$.

transformations. The best combination of features we found is gathered in Table I, which makes a total of 4δ measurements. Here, Cpk and Vpk have been combined into a single feature.

The logistic regression algorithm has been evaluated for different δ values, with 60% of the data set for training, 20% for cross-validation, and 20% for testing. The subsets were created randomly from the examples in the data set. Fig. 4(a) shows the success rate of the classification task for the test subset with the logistic regression algorithm, as a function of δ. It can be seen that values of δ above 10 do not improve the accuracy of the method, while additional measurements further reduce the RUL of the cell. Thus, we will only consider the case of $\delta = 10$ in the rest of the analysis. Fig. 4(b) shows the confusion matrix for this case.

The overall accuracy in the classification obtained with this method is around 97.27%, with 93.7% accuracy for detecting "Short RUL cells" and 98.1% accuracy for "Long RUL cells." We emphasize that we achieve this high accuracy for cells in an unknown moment of their life, i.e., we do not know how many cycles they have been used before the measurement tests.

IV. RUL REGRESSION

After observing the classification capabilities of the features, we would like to know how well they are capable of performing actual RUL estimation, i.e., predicting the specific number of remaining cycles for a given cell. For this purpose, as an initial approach, multivariable linear regression (MLR) is considered.

A. Direct RUL Estimation Approach

The first RUL regression method that we consider is the MLR algorithm. We use 60% of the data set for training, while 20% is used for cross-validation and 20% for testing. The predicted output of this algorithm for a given measurement input array is given by the following expression:

$$\hat{y}(\boldsymbol{x}, \boldsymbol{w}) = \boldsymbol{w}^T \boldsymbol{x} \tag{5}$$

where $\hat{y}$ is the predicted RUL, $\boldsymbol{x}$ is a $4\delta+1$ dimensional measurement array, and $\boldsymbol{w}$ is a $4\delta + 1$ dimensional weight array (due to the bias term). The algorithm fits $\boldsymbol{w}$ by minimizing the cost function J in the following equation:

$$J(\boldsymbol{w}) = \frac{1}{2m}\sum_{i=1}^{m}\left(\boldsymbol{w}^T \boldsymbol{x}_i - y_i\right)^2 + \lambda \sum_{j=1}^{n} \boldsymbol{w}_j^2 \tag{6}$$

where the first term is the traditional least-squares function and the second term is the Ridge regularization function, introduced to avoid overfitting as in the case of the classification problem. Again, the parameter m is the number of training examples and λ, the regularization weight.

To select from the 40 features those that are more relevant for regression purposes, the sequential forward selection (SFS) and sequential backward selection (SBS) algorithms have been used [34]–[36]. The SFS method starts with an empty set of measurements and evaluates each of them independently, selecting the one that performs the best, and then, saves it and adds each of the other measurements, selecting the one that performs the best. The algorithm keeps on selecting measurements until all of them have been added, and then, selects the iteration with less error as the best performing mix of features. The SBS method does something similar, but starting with a full data set and evaluating the error when each measurement is removed. Those that have less impact on the error are less important, and keep on being eliminated. Each simulation of the algorithms gave different results due to the random generation of the training, validation, and test subsets. However, two common aspects have been observed:

1) The performance of both algorithms in their optimum points is always similar.
2) The best performance versus the number of measurements tradeoff is obtained when including just one measurement for each type of feature. The performance can be slightly increased when adding more measurements. Specifically, IR seems to be the least important feature in that regard, and most of its measurements can be omitted.

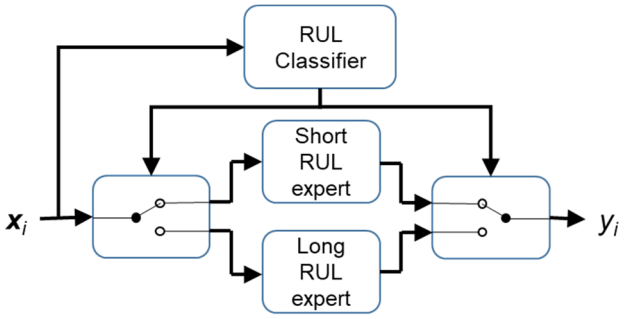

Fig. 5. MES scheme, where the RUL classifier acts as a selector of the expert.

The best performance in these algorithms is obtained when including the first 36 measurements for the SFS algorithm. The variables finally discarded are IR_1, IR_2, IR_4, and IR_8, all of them, among the ten measurements of Internal Resistance. They seem to provide redundant information, which is already given by other IR measurements.

As an alternative to MLR, some more sophisticated algorithms have been considered. One of these algorithms is the multilayer perceptron (MLP) (or feed-forward neural network). The inputs to this algorithm are the same as for the case of MLR. This algorithm has been trained using the Levenberg-Marquardt optimization algorithm with $\mu_0 = 10^{-3}$ and the mean squared error (MSE) as the optimization goal, for a maximum of 1000 epochs with early stopping as a validation technique. A single hidden layer has been used, and the number of neurons in the said layer has been swept. The optimal was found at 32 neurons.

The algorithms have been trained with the whole data set (maintaining 60% for training, 20% for validation, and 20% for test). However, after observing the accuracy in the classification problem, we conclude that the "Short RUL" and "Long RUL" classes have a clear different behavior. Thus, we propose "expert" algorithms, which have been trained and tested with two different subsets: one for short RUL cells (those below 150 RUL cycles) and the other for long RUL cells (those above 150 RUL cycles). These expert algorithms have been combined in the multiple expert system (MES) (Fig. 5), where the "RUL Classifier" block (the logistic regression algorithm described in Section III) chooses which expert to use after classifying the input vector in one of the classes. Once the expert has been chosen, the input is fed to such expert (either "Short RUL expert" or "Long RUL expert"), thus obtaining the final output.

The test results for the algorithms are collected in Table II. The error metrics are provided in terms of root mean square error (RMSE) and mean relative error (MRE) in the following equations:

$$\text{RMSE} = \sqrt{\frac{1}{m}\sum_{i=1}^{m}(\hat{y}_i - y_i)^2} \tag{7}$$

$$\text{MRE} = \frac{1}{m}\sum_{i=1}^{m}\frac{(\hat{y}_i - y_i)}{y_i}\cdot 100(\%) \tag{8}$$

TABLE II
ERROR METRICS FOR DIFFERENT ALGORITHMS

Algorithm	RMSE (cycles)	MRE (%)	MRE (%) (>150 cycles)
Global MLR	90	53.81	18.51
Global MLP	52	23.03	10.51
MLP Short RUL expert (<150 cycles)	13	28.73	-
MLP Long RUL expert (>150 cycles)	61	10.32	10.32
MES	49	15.2	9.79
Elastic Net	86	10.1	-

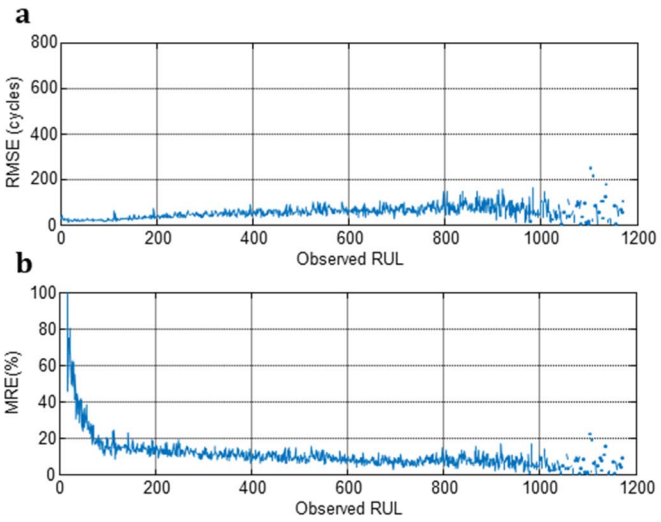

Fig. 6. Error rates for the MLP algorithm versus observed RUL. (a) RMSE. (b) MRE.

where m is the number of examples in the test data set, $\hat{y}_i$ is the predicted RUL for the ith example, and y_i is the actual RUL values for the ith example.

In the table, the algorithms labeled as "global" are those trained with the whole data set (maintaining 60% for training, 20% for cross-validation, and 20% for test). Although some of these error rates may seem unimpressive, especially in the case of MRE near 50%, cells with very low RUL (only a few cycles) have a large impact on this averaged error. A small error of only a few cycles for cells with low RUL (e.g., one of two cycles) leads to a large MRE. To clarify this, Fig. 6 provides information on the RMSE and MRE obtained for each value of observed RUL. Note that in the case of the MRE [Fig. 6(b)], the error is within 10%–20% for practically the whole range of observed RUL. It can be seen that MRE is not a good representation of the method on the first 100 cycles. The third column in the table gives MRE conditioned on larger values of RUL, which yields much better MRE results.

The results for the MES are given in the table, where it may be appreciated how it enhances the performance of the global algorithm, obtaining an average MRE of 15.2% in the estimation of RUL for cells in an unknown moment of their life, and below 10% conditioned to long RUL cells. Fig. 7 shows an example of RUL estimation for all of the test cycles

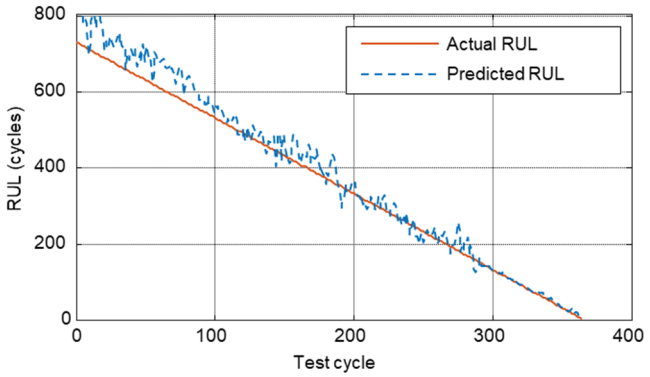

Fig. 7. RUL estimate with MES for all the cycles belonging to cell #100.

for one specific cell in the data set (#100). It can be appreciated how the RUL prediction curve follows accurately the RUL line. This is especially noticeable for low RUL values, where the Short Expert comes into play (below 150 RUL cycles), where despite the higher MRE the absolute prediction is much more accurate.

As a means of comparison, the last row of the table collects the RUL estimation error from the Elastic Net algorithm developed in [27] with the same data set, which used the linear regression framework. The results in terms of RMSE are closer to the MLR algorithm. It must be noted that the approach followed in that reference is not the same that has been followed here since they used information from the first 100 cycles of each cell. This has an impact on the lower MRE since they do not try to predict very low RUL values.

B. Capacity Prediction Approach

In the problem of capacity prediction, the algorithm will predict the future capacity of the cell, after a set number of cycles ahead from the cycle where the features have been measured. As test examples, we have considered 100, 150, and 200 cycles ahead. The closer the prediction horizon is located, the more accurate will be the prediction. The same features as in the RUL estimation algorithm have been chosen. Besides, different δ values for the measurement cycles have been considered. Since MLP had obtained the best results among the global algorithms, it has been chosen for this task. The results are shown in Table III.

The accuracy in the prediction of capacity is very high according to the MRE metrics obtained. Among the δ and cycles ahead values that have been tested, the best MRE obtained is 0.24%. However, a higher window observation δ or a closer prediction horizon provides better error figures. As an example, Fig. 8 shows the output for cell #100 in the data set, when predicting capacity 150 cycles ahead of the measurement moment.

Observing the accurate capacity prediction results, we wonder if there is a possibility of using this algorithm for RUL estimation purposes. In this scenario, we define an EoL condition based on capacity (e.g., 80% of nominal capacity) and we train algorithms to predict cell capacity X cycles ahead. We keep track of the battery along with its life, and when the prediction falls below the EoL condition, we predict RUL as X cycles. Table IV shows the accuracy in this RUL prediction method, which is higher than for the case of the MES algorithm but with a fixed number of cycles ahead.

TABLE III
ERROR RESULTS FOR CAPACITY PREDICTION

Cycles ahead	δ	MRE (%)
100	1	0.45
	10	0.24
150	1	0.67
	10	0.45
200	1	0.82
	10	0.64

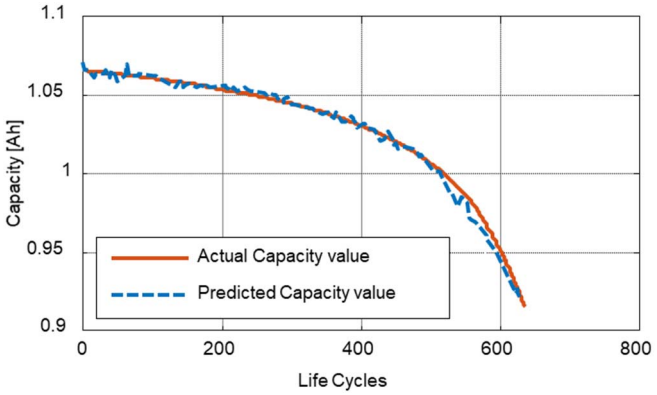

Fig. 8. Capacity prediction for cell #100 after 150 cycles.

TABLE IV
ERROR RESULTS FOR RUL PREDICTION BASED ON CAPACITY

Cycles ahead	MRE (%)
100	6.9
150	8.6
200	9.99

C. Indirect RUL Estimation Approach

So far, we have described the study of the RUL estimation problem from a Direct Estimation approach, meaning that capacity measurements are available as a feature for further analysis. This is meaningful from the second-life application perspective since we are conducting some test cycles to a cell in a controlled environment and it can be charged and discharged at will.

However, it is interesting to see how well these features can perform in other scenarios, e.g., a system where the battery cannot be completely discharged for test purposes, such as in an UPS. In these systems, direct measurement of capacity and other capacity-related features are generally unavailable and thus, RUL estimation algorithms must do as best as they can with a subset of features. This has been introduced as "Indirect RUL Estimation" in the literature [19], [28].

TABLE V
ERROR RESULTS FOR MES IN INDIRECT ESTIMATION

Algorithm	RMSE (cycles)	MRE (%)	MRE (%) (>150 cycles)
MES	109	45.19	23.94

Thus, from the features we have been considering until now, Capacity and ΔC are not suitable for this approach. Even more, capacitance peak-related features (Vpk, Cpk) should not be considered as well (they are found in the last 10% of SoC). For this reason, only TIEDVD and IR features are considered for this approach. From the algorithms that have already been introduced, the MES performs the best. The RMSE and MRE metrics are contained in Table V. The error metrics are far from those obtained in the Direct Estimation approach, but still may be of interest in these applications.

V. CONCLUSION

RUL estimation is becoming a popular topic in battery-related research. Due to the complexity of the problem, data-driven approaches are appropriate for the task, although until very recently, publicly available data sets were small and simple. We address the problem of RUL estimation from the second-life application point of view. The main hypothesis assumes that past information about cell use is not available. By conducting some simple charge and discharge tests and analyzing the voltage waveforms, we can determine the number of RUL cycles with high accuracy. For this purpose, we have proposed several HI to be analyzed. Among them, there are well-known features such as Capacity or Internal Resistance, previously described features such as TIEDVD, and two novel HI (C_{peak}, V_{peak}), which have been observed in this specific data set.

We propose some simple but effective algorithms to classify used cells into "Short RUL" and "High RUL" categories with an average accuracy higher than 97%. We also proposed methods to estimate the exact number of remaining cycles for cells in an unknown moment of their lives, with 49 cycles of rms error, providing an overall MRE of 15.2% and 9.79% for high RUL cells. In the capacity prediction problem, we obtain high accuracy when predicting the future value in a set amount of cycles, with relative errors below 1% in all the studied scenarios. As the last contribution, we study the viability of performing indirect estimation in embedded applications with a subset of features, obtaining approximate values for the RUL of these cells. The high accuracy in the prediction of short RUL cells (highly decayed and not useful) makes this approach a suitable method for determining whether a cell would be useful for a second-life application such as grid-oriented ESS. On top of this, the prediction of the exact number of RUL cycles is made with high accuracy and is considered good for this purpose.

This work has been developed with the data set by TRI since it is the most complete in terms of the number of cells and cycles among the data sets currently available. Even though this approach would be valid for determining the RUL of any chemistry and type of cell, a specific data set would be needed for said kind of cell to be able to train the algorithms. In addition, the applicability of the novel HI described in the article would need to be researched for other chemistries, which is a subject for future work.

In addition, future lines of work also include developing advanced algorithms, to enhance the prediction of RUL and the classification of the cells.

REFERENCES

[1] B. Nykvist and M. Nilsson, "Rapidly falling costs of battery packs for electric vehicles," *Nature Climate Change*, vol. 5, no. 4, pp. 329–332, Apr. 2015, doi: 10.1038/nclimate2564.

[2] B. Dunn, H. Kamath, and J.-M. Tarascon, "Electrical energy storage for the grid: A battery of choices," *Science*, vol. 334, no. 6058, pp. 928–935, Nov. 2011, doi: 10.1126/science.1212741.

[3] B. Diouf and R. Pode, "Potential of lithium-ion batteries in renewable energy," *Renew. Energy*, vol. 76, pp. 375–380, Apr. 2015, doi: 10.1016/j.renene.2014.11.058.

[4] S. B. Peterson, J. Apt, and J. F. Whitacre, "Lithium-ion battery cell degradation resulting from realistic vehicle and vehicle-to-grid utilization," *J. Power Sour.*, vol. 195, no. 8, pp. 2385–2392, Apr. 2010, doi: 10.1016/J.JPOWSOUR.2009.10.010.

[5] K. Young, C. Wang, L. Y. Wang, and K. Strunz, "Electric vehicle battery technologies," in *Electric Vehicle Integration into Modern Power Networks*. New York, NY, USA: Springer, 2013, pp. 15–56.

[6] C. Ioakimidis, A. Murillo-Marrodán, A. Bagheri, D. Thomas, and K. Genikomsakis, "Life cycle assessment of a lithium iron phosphate (LFP) electric vehicle battery in second life application scenarios," *Sustainability*, vol. 11, no. 9, p. 2527, May 2019, doi: 10.3390/su11092527.

[7] M. Farhadi and O. Mohammed, "Energy storage technologies for high-power applications," *IEEE Trans. Ind. Appl.*, vol. 52, no. 3, pp. 1953–1961, May 2016, doi: 10.1109/TIA.2015.2511096.

[8] D. Ansean, M. Gonzalez, J. C. Viera, J. C. Alvarez, C. Blanco, and V. M. Garcia, "Evaluation of $LiFePO_4$ batteries for electric vehicle applications," in *Proc. Int. Conf. New Concepts Smart Cities, Fostering Public Private Alliances (SmartMILE)*, Dec. 2013, pp. 1–8, doi: 10.1109/SmartMILE.2013.6708211.

[9] R. Reinhardt, I. Christodoulou, S. Gassó-Domingo, and B. A. García, "Towards sustainable business models for electric vehicle battery second use: A critical review," *J. Environ. Manage.*, vol. 245, pp. 432–446, Sep. 2019, doi: 10.1016/J.JENVMAN.2019.05.095.

[10] E. Martinez-Laserna *et al.*, "Battery second life: Hype, hope or reality? A critical review of the state of the art," *Renew. Sustain. Energy Rev.*, vol. 93, pp. 701–718, Oct. 2018, doi: 10.1016/J.RSER.2018.04.035.

[11] Y. Jiang, J. Jiang, C. Zhang, W. Zhang, Y. Gao, and N. Li, "State of health estimation of second-life $LiFePO_4$ batteries for energy storage applications," *J. Cleaner Prod.*, vol. 205, pp. 754–762, Dec. 2018, doi: 10.1016/J.JCLEPRO.2018.09.149.

[12] E. Hossain, D. Murtaugh, J. Mody, H. M. R. Faruque, M. S. H. Sunny, and N. Mohammad, "A comprehensive review on second-life batteries: Current state, manufacturing considerations, applications, impacts, barriers & potential solutions, business strategies, and policies," *IEEE Access*, vol. 7, pp. 73215–73252, 2019, doi: 10.1109/ACCESS.2019.2917859.

[13] R. B. Wright *et al.*, "Power fade and capacity fade resulting from cycle-life testing of advanced technology development program lithium-ion batteries," *J. Power Sour.*, vols. 119–121, pp. 865–869, Jun. 2003, doi: 10.1016/S0378-7753(03)00190-3.

[14] M. Broussely, S. Herreyre, P. Biensan, P. Kasztejna, K. Nechev, and R. Staniewicz, "Aging mechanism in Li ion cells and calendar life predictions," *J. Power Sour.*, vols. 97–98, pp. 13–21, Jul. 2001, doi: 10.1016/S0378-7753(01)00722-4.

[15] I. Bloom *et al.*, "An accelerated calendar and cycle life study of Li-ion cells," *J. Power Sour.*, vol. 101, no. 2, pp. 238–247, Oct. 2001, doi: 10.1016/S0378-7753(01)00783-2.

[16] S. F. Schuster *et al.*, "Nonlinear aging characteristics of lithium-ion cells under different operational conditions," *J. Energy Storage*, vol. 1, pp. 44–53, Jun. 2015, doi: 10.1016/J.EST.2015.05.003.

[17] H. Chaoui and C. C. Ibe-Ekeocha, "State of charge and state of health estimation for lithium batteries using recurrent neural networks," *IEEE Trans. Veh. Technol.*, vol. 66, no. 10, pp. 8773–8783, Oct. 2017, doi: 10.1109/TVT.2017.2715333.
[18] S. Sepasi, R. Ghorbani, and B. Y. Liaw, "Inline state of health estimation of lithium-ion batteries using state of charge calculation," *J. Power Sour.*, vol. 299, pp. 246–254, Dec. 2015, doi: 10.1016/j.jpowsour.2015.08.091.
[19] D. Liu, W. Xie, H. Liao, and Y. Peng, "An integrated probabilistic approach to lithium-ion battery remaining useful life estimation," *IEEE Trans. Instrum. Meas.*, vol. 64, no. 3, pp. 660–670, Mar. 2015, doi: 10.1109/TIM.2014.2348613.
[20] L. Li, Y. Peng, Y. Song, and D. Liu, "Lithium-ion battery remaining useful life prognostics using data-driven deep learning algorithm," in *Proc. Prognostics Syst. Health Manage. Conf. (PHM-Chongqing)*, Oct. 2018, pp. 1094–1100, doi: 10.1109/PHM-Chongqing.2018.00193.
[21] R. Khelif, B. Chebel-Morello, S. Malinowski, E. Laajili, F. Fnaiech, and N. Zerhouni, "Direct remaining useful life estimation based on support vector regression," *IEEE Trans. Ind. Electron.*, vol. 64, no. 3, pp. 2276–2285, Mar. 2017, doi: 10.1109/TIE.2016.2623260.
[22] D. Liu, H. Wang, Y. Peng, W. Xie, and H. Liao, "Satellite lithium-ion battery remaining cycle life prediction with novel indirect health indicator extraction," *Energies*, vol. 6, no. 8, pp. 3654–3668, Jul. 2013, doi: 10.3390/en6083654.
[23] C. Chen and M. Pecht, "Prognostics of lithium-ion batteries using model-based and data-driven methods," in *Proc. IEEE Prognostics Syst. Health Manage. Conf. (PHM)*, May 2012, pp. 1–6, doi: 10.1109/PHM.2012.6228850.
[24] J. Liu and Z. Chen, "Remaining useful life prediction of lithium-ion batteries based on health indicator and Gaussian process regression model," *IEEE Access*, vol. 7, pp. 39474–39484, 2019, doi: 10.1109/ACCESS.2019.2905740.
[25] E. Martinez-Laserna *et al.*, "Technical viability of battery second life: A study from the ageing perspective," *IEEE Trans. Ind. Appl.*, vol. 54, no. 3, pp. 2703–2713, May 2018, doi: 10.1109/TIA.2018.2801262.
[26] L. Ren, L. Zhao, S. Hong, S. Zhao, H. Wang, and L. Zhang, "Remaining useful life prediction for lithium-ion battery: A deep learning approach," *IEEE Access*, vol. 6, pp. 50587–50598, 2018, doi: 10.1109/ACCESS.2018.2858856.
[27] K. A. Severson *et al.*, "Data-driven prediction of battery cycle life before capacity degradation," *Nature Energy*, vol. 4, no. 5, pp. 383–391, May 2019, doi: 10.1038/s41560-019-0356-8.
[28] L. Li, Y. Zhu, L. Wang, D. Yue, and D. Li, "Indirect remaining useful life prognostics for lithium-ion batteries," in *Proc. 24th Int. Conf. Automat. Comput.*, Sep. 2018, pp. 1–5, doi: 10.23919/iconac.2018.8748973.
[29] M. Günther, U. Feldmann, and J. T. Maten, "Modelling and discretization of circuit problems," *Handbook Numer. Anal.*, vol. 13, pp. 523–659, Jan. 2005, doi: 10.1016/S1570-8659(04)13006-8.
[30] J. L. Wyatt, *Foundations of Nonlinear Network Theory*. Berkeley, CA, USA: Univ. of California, Berkeley, 1978.
[31] J. Macdonald and M. Brachman, "The charging and discharging of nonlinear capacitors," *Proc. IRE*, vol. 43, no. 1, pp. 71–78, 1955, doi: 10.1109/JRPROC.1955.277920.
[32] D. Ansean *et al.*, "Lithium-ion battery degradation indicators via incremental capacity analysis," *IEEE Trans. Ind. Appl.*, vol. 55, no. 3, pp. 2992–3002, May 2019, doi: 10.1109/TIA.2019.2891213.
[33] E. Martinez-Laserna *et al.*, "Evaluation of lithium-ion battery second life performance and degradation," in *Proc. IEEE Energy Convers. Congr. Expo. (ECCE)*, Sep. 2016, pp. 1–7, doi: 10.1109/ECCE.2016.7855090.
[34] M. Dash and H. Liu, "Feature selection for classification," *Intell. Data Anal.*, vol. 1, nos. 1–4, pp. 131–156, 1997. [Online]. Available: https://www.elsevier.comAocate/ida
[35] P. A. Devijver and J. Kittler, *Pattern Recognition: A Statistical Approach*. Upper Saddle River, NJ, USA: Prentice-Hall, 1982.
[36] R. Kohavi and G. H. John, "Wrappers for feature subset selection," *Artif. Intell.*, vol. 97, nos. 1–2, pp. 273–324, Dec. 1997, doi: 10.1016/S0004-3702(97)00043-X.

Iván Sanz-Gorrachategui received the B.Sc. and M.Sc. degrees in electrical engineering from the University of Zaragoza, Zaragoza, Spain, in 2015 and 2016, respectively, where he is currently pursuing the Ph.D. degree with the Power Electronics and Micro-Electronics Group.

In 2019 and 2020, he was a Fulbright Scholar with the Mitsubishi Electric Research Laboratories, Cambridge, MA, USA. His current research interests include high-efficiency resonant switch-mode converters, energy storage systems, and machine-learning algorithms applied to their controllability.

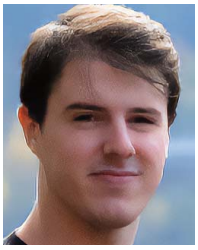

Pablo Pastor-Flores received the B.Sc. and M.Sc. degrees in electrical engineering from the University of Zaragoza, Zaragoza, Spain, in 2018 and 2019, respectively, where he is currently pursuing the Ph.D. degree in machine learning techniques applied to energy systems.

His current research interests are focused on unsupervised learning, state of health (SOH) algorithms, and battery aging.

Milutin Pajovic (Member, IEEE) received the Dipl.-Ing. degree in electrical engineering from the University of Montenegro, Podgorica, Montenegro, in 2005, the M.S. degree in ocean engineering from Florida Atlantic University, Boca Raton, FL, USA, in 2009, and the Ph.D. degree in electrical and oceanographic engineering from the Massachusetts Institute of Technology and Woods Hole Oceanographic Institution, Cambridge, MA, USA, in 2014.

He was a Research Intern with the Mitsubishi Electric Research Laboratories (MERL), Cambridge, and ExxonMobil's Upstream Research Company, Houston, TX, USA, in Summers 2013 and 2012. From September 2014 to January 2020, he has been with MERL in the role of a Principal Research Scientist. He is currently a Senior Research Scientist with Analog Devices Inc., Boston, MA. His current research interests include signal processing, machine learning, and wireless communications.

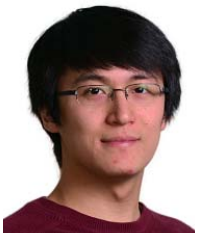

Ye Wang received the B.S. degree in electrical and computer engineering from the Worcester Polytechnic Institute, Worcester, MA, USA, in 2005, and the M.S. and Ph.D. degrees in electrical and computer engineering from Boston University, Boston, MA, in 2009 and 2011, respectively.

In 2012, he joined Mitsubishi Electric Research Laboratories, Cambridge, MA, where he had also previously completed an Internship in 2010. His current research interests include information theory, machine learning, signal processing, communications, and data privacy/security.

Philip V. Orlik (Senior Member, IEEE) received the B.E. and M.S. degrees from the State University of New York (SUNY) at Stony Brook, Stony Brook, NY, USA, in 1994 and 1997, respectively, where he received the Ph. D. degree in electrical engineering, in 1999.

From 1999 to 2000, he was a Simulation and Modeling Engineer with the Mitre Corporation, McLean, VA, USA. In 2000, he joined Mitsubishi Electric Research Laboratories (MERL), Inc., Cambridge, MA, USA, as a Member of Technical Staff. He is currently the Manager of the Signal Processing Group. His current research interests focused on advanced signal processing methods for various applications including radar, material sensing, advanced wireless and wired communications, sensor, and the Internet of Things (IoT) networks. Other research interests include vehicular/car-to-car communications, mobility modeling, performance analysis, and queuing theory.

Carlos Bernal-Ruiz (Member, IEEE) received the M.Sc. and Ph.D. degrees in electrical engineering from the University of Zaragoza, Zaragoza, Spain, in 2000 and 2012, respectively.

Since 2001, he has been an Associate Professor, with a special interest in power and mixed-signal electronics, with the University of Zaragoza. His current research interests are focused on high-efficiency resonant switch-mode converters and their control.

Antonio Bono-Nuez received the M.Sc. and Ph.D. degrees in electronic engineering from the University of Zaragoza, Zaragoza, Spain, in 2008 and 2016, respectively.

Since 2001, he has been an Associate Professor of electronic engineering with the University of Zaragoza. He has authored over two patents and more than 35 papers and congress communications. His current research interests include microprocessors and machine learning in energy storage systems.

Jesús Sergio Artal-Sevil received the B.Sc. degree in electrical engineering from the University of Zaragoza, Zaragoza, Spain, in 1997, and the M.Sc. degree in renewable energy and energy efficiency and the M.Sc. degree in electronic engineering both from the University of Zaragoza, in 2014 and 2016, respectively.

He worked in the automotive industry as a Design and Development Engineer in the vehicle electrical and electronic technology division from 1997 to 2001. Since then, he has participated in various research projects in the fields of renewable energy applications, energy storage applications, and off-grid systems. He is currently a Researcher and Full-Time Professor with the Department of Electrical Engineering, Faculty of Engineering, University of Zaragoza. Currently, he is the author or coauthor of more than 100 scientific papers on journals and conferences. His current research interests include power electronics, resonant and soft-switched power converters, modeling and control of converters, solid-state transformers, flexible alternating current transmission systems (FACTS), and power conversion applications.